DOI: 10.35595/2414-9179-2020-2-26-421-435

Hemalatha Gonuguntla[1]**, Khudoyberdi A. Abdivaitov**[2]**, Mahalingam Bose**[3]**, Muzaffar E. Rakhmataliev**[4]

A COMPARISON OF SENTINEL-1 AND SENTINEL- 2 IN ASSESSING FLOODED AREA AND BUILT-UP LAND USE: A CASE STUDY OF SELECTED COASTAL DISTRICTS IN ANDHRA PRADESH, INDIA

ABSTRACT

In tropical climatic conditions, floods occur during heavy rainfall. Floods during this thick cloud cover partially stops the optical imagery to pass through the atmosphere and record the surface reflectance. Another kind of satellite imagery that is available is microwave remote sensing data that can pass through the clouds. However, the exploration of this microwave remote sensing began recently for earth observation applications. So, the algorithms and methods available for exploiting advantages from microwave data is still under research. The current part of the work is to explore the methods available to differentiate between the microwave data (Sentinel-1) and Optical imagery (Sentinel-2) in flooded and built-up area estimation. The ultimate aim is to conclude with most suitable datasets and fast computing methods in estimating the built-up area and flooded area during the emergency disaster time. Two case studies taken up for the study are August 2019 East Godavari floods and October 2019 Titli cyclone. So, the adopted method to estimate the flooded areas and built-up areas from the Sentinel-1A and Sentinel-2B was RGB clustering (Red, Green and Blue clustering) using the derived RGB colour combinations in snap 7.0 software. The datasets were classified into built-up, flooded area and vegetation areas using Random Forest supervised classification, a machine learning technique Validation of estimated built-up and flooded areas estimated from Sentinel-1A and Sentinel-2B was done using the random pixel distribution technique. Since the de-centralisation of estimated flooded areas and built-up area helps in fast distribution of the response forces to the affected area, estimation of built-up and flooded area was also taken up for the sub-districts of East Godavari district, India. Finally, the study estimates the damaged built-up and vegetation due to August 2019 East Godavari floods from Sentinel-1A and Sentinel-2B. Flooded area due to 'Titli' cyclone 2018 was estimated in East Godavari, Visakhapatnam and Vijianagaram districts of Andhra Pradesh state.

KEYWORDS: Microwave remote sensing, optical remote sensing, RGB clustering, Random Forest supervised classification, damage estimation

INTRODUCTION

The current work is centred at exploration of differences between sentinel-1 and sentinel-2 in terms of methodology and estimation of built-up and flooded areas. The current research extends the RGB combinations exploration towards flooded areas estimation in Sentinel-2 and built-up area estimation in Sentinel-1 from previous research work of flooded area estimation in Sentinel-1 and built-up area estimation in Sentinel-2 respectively. 2014 Uttarakhand floods and

[1] Central University of Karnataka (CUK), Kadaganchi, Aland Road, 585367, Kalaburagi Dist., Karnataka, India; *e-mail:* **hemagonuguntla@gmail.com**

[2] Tashkent Institute of Irrigation and Agricultural Mechanization Engineers (TIIAME), Kari Niyaziy str., 39, 100000, Tashkent, Uzbekistan; *e-mail:* **abdivaitov90@list.ru**

[3] Central University of Karnataka (CUK), Kadaganchi, Aland Road, 585367, Kalaburagi Dist., Karnataka, India; *e-mail:* **mahabose@gmail.com**

[4] Tashkent Institute of Irrigation and Agricultural Mechanization Engineers (TIIAME), Kari Niyaziy str., 39, 100000, Tashkent, Uzbekistan; *e-mail:* **m.raxmataliyev@tiiame.uz**

August 2019 floods in East Godavari district of Andhra Pradesh state in India, revealed that the rivers in tropical regions are dynamic. There are two major ways to rescue people from flood. First to save immediately after flood and second is encouraging people to build residences in flood resilient places which are of immediate and gradual methods respectively. Hence the reason for India there are rescue teams and flood analysis teams jointly working for flood risk management. Since the existence of dynamic weather phenomenon, emphasis shall be on rescue operations during flood time unlike on replacing residences to flood resilient locations. Hence the reason for the current research is on fast computable and reliable method in mapping flooded areas to support in emergency times.

To obtain the spatial and temporal information of earth's surface elements like built-up areas, vegetation, flooded areas and water bodies, major methods existed are field survey, airborne remote sensing and satellite remote sensing. Every year thousands of people losing their livelihoods, huge damage to infrastructure due to cyclones leading billions of economic losses to Andhra Pradesh state of India. Assessing the damage occurred immediately after cyclone ensures the early redressal mechanisms from the government to stabilise the livelihoods of people as soon possible. This motivated the current research to study about the damage assessment due to cyclones over Andhra Pradesh state. Andhra Pradesh was selected as a study because, among three states (Odisha, Andhra Pradesh and Tamilnadu) affected due to cyclone at east coast of India, AP is at centre of them, running into huge economic loss every year compare to other states. The urban areas are also expanding at a rapid pace with congested streets, clustered settlements, concentrated infrastructure and dense population. Due to the presence of these elements in urban areas, field survey is highly difficult in terms of time and work for estimating the damage due to disaster. Hence remote sensing, sensing from far, plays a very important role in assessing damage in terms of its capacity to cover a vast area in one acquisition time and high-resolution acquisition capability at economically viable price [*Joyce et al.*, 2009; *Klemas*, 2009]. These remote sensing capabilities in times of disaster emergency, motivated the current research towards exploration of different remote sensing datasets and their differences in capabilities in estimating the flooded areas, built-up areas, vegetation and water bodies. The ultimate aim is to assess the damage caused by Cyclones in Andhra Pradesh state, India. Damage in terms of built-up area, vegetation, and inundated area using SAR and Optical imagery. The aim of the current research is to find out advantages and limitations of a S-1A (microwave remote sensing satellite data) and S-2B (optical remote sensing satellite data) in estimating built-up, flooded and vegetation areas. Finally, to explore the fast computing methods, so that disaster response forces can mitigate computing time and hence more time can be invested in rescue tasks (fig. 1).

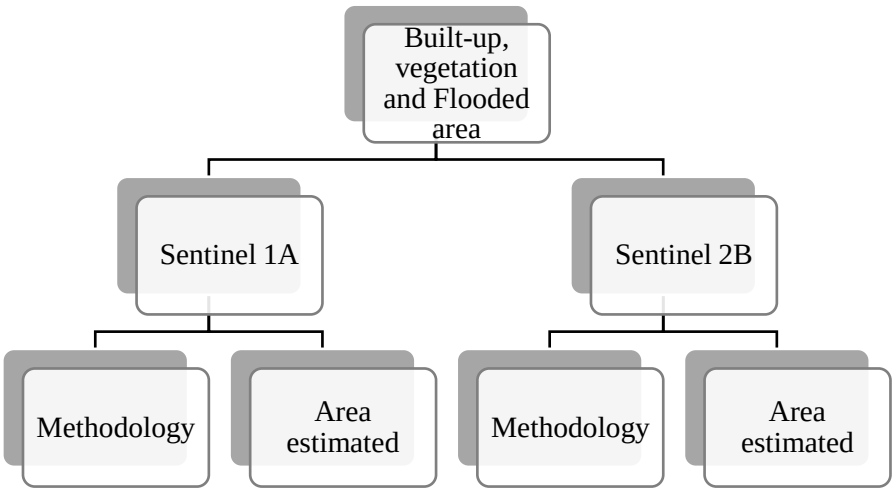

Fig. 1. Displaying the aim of current work

The main objectives of this research are:

- Analysing time and dates of 2018 Titli cyclone and 2019 August floods (in East Godavari district) that affected the Andhra Pradesh state for data acquisition.
- Exploring differences in methods between Sentinel-1A and Sentinel-2B in estimation of flooded areas, built-up and vegetation areas.
- Damaged area estimation of Built-up area, vegetation due to august 2019 EG floods. Flooded areas due to 2018 Titli cyclone in East Godavari, Visakhapatnam and Vizianagaram districts of Andhra Pradesh state and August 2019 floods in East Godavari district of Andhra Pradesh state.
- Accuracy assessment of the results obtained.

Study area for Titli cyclone is East Godavari, Visakhapatnam and Vizianagaram districts of Andhra Pradesh state, India. Study area for 2019 August East Godavari floods is East Godavari district (fig. 2).

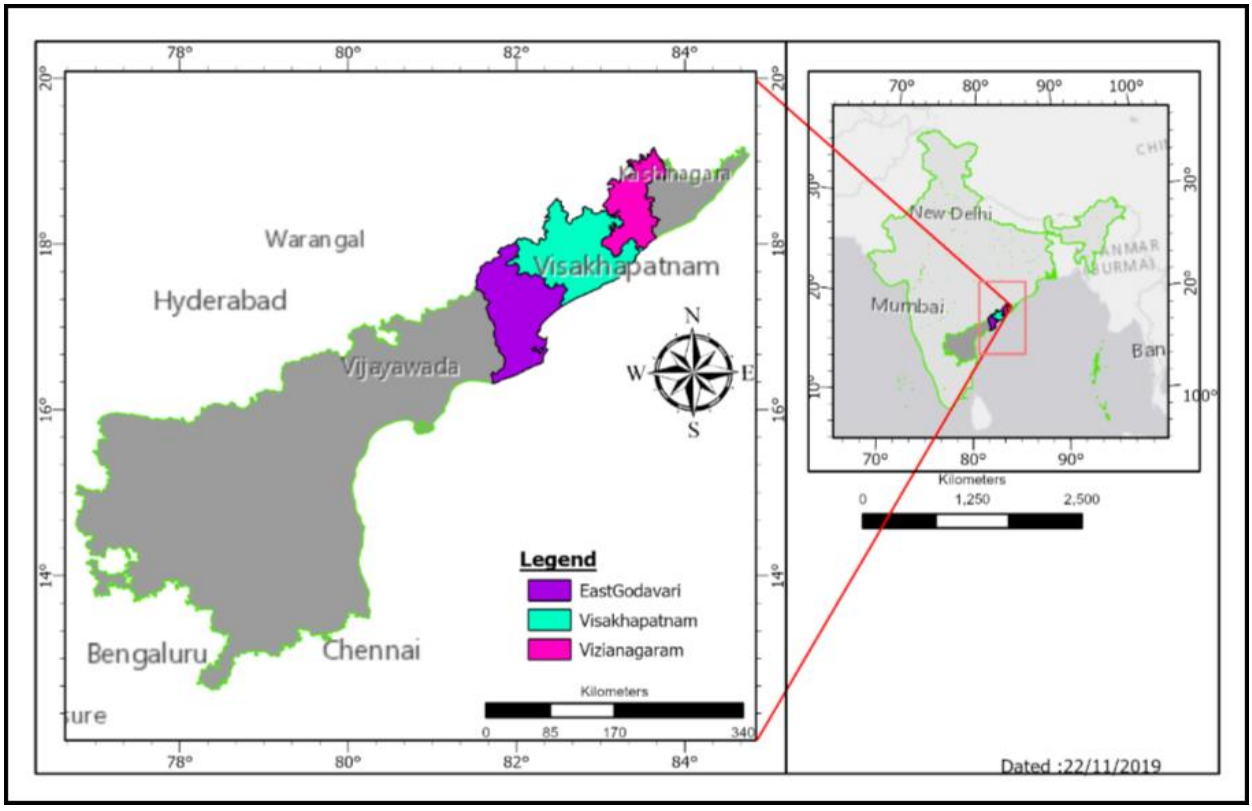

Fig. 2. Study area of the current work

The chapter of the background information details about conceptual understanding on floods, Cyclone, built-up area. Then it details about the current practices of flood, built-up areas estimation. Finally, it details about two case studies that were taken up currently and distinguishing the two different datasets namely Sentinel-1A, which is microwave remote sensing data and Sentinel-2B, which is optical remote sensing data.

The continuous heat of water forms water vapor. The water vapor converts to water during rains and the heat get released to the atmosphere. This released heat warms up the surrounding air and makes it move up thereby decreasing the pressure. This low-pressure area attracts the high-pressure winds around. This cycle repeats until a low-pressure system surrounded by high speed winds. This system is called cyclone. Tropical cyclones which formed over warm ocean basins from which they intensify into severe to very severe cyclones. One such

very severe cyclone 'HUDHUD' that hit east coast of Andhra Pradesh state in 2014 left huge economic loss besides human loss [*Jain*, 2015]. Flood is an overflow of huge amount of water upon dry land by crossing normal limits. In India, millions of human lives, cattle and agricultural crops are being destroyed due to lack of planning and improper weather forecasting *[Saptarsi et al.*, 2018]. Flood usually crosses the distances at a greater speed ad increases with greater heights. Hence every minute counts in rescue operations. Any delay in identifying the flood areas and sometimes predicting the flood areas may cost a life.

East Godavari district located at East bank of Godavari river in Andhra Pradesh state, India. It got affected by the severe floods occurred during first week of the August 2019. Heavy and incessant rainfall lead the flood water from Godavari river to cross river banks and inundate the nearby districts. Hence this is our first current study to compare the flood area estimation between the Sentinel-1A and Sentinel-2B data sets [*Pradesh*, 2019].

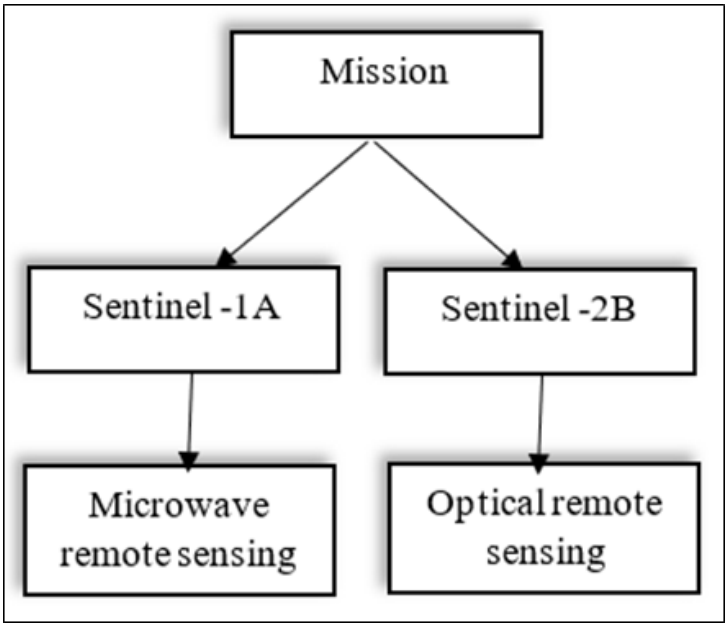

Fig. 3. Difference between the S-1A & S-2B

Among the different types of remote sensing (RS), microwave RS and optical RS are the two RS types most popularly advancing into the estimation of built-up and flooded areas. European Space Agency (ESA) launched two major satellites name Sentinel-1 and Sentinel-2. Sentinel-1 is a combo of two satellites namely Sentinel-1A (S-1A) and Sentinel-1B (S-1B) which are the sensors of microwave remote sensing. Sentinel-2 is a combo of two satellites namely Sentinel-2A (S-2A) and Sentinel-2B (S-2B) which are the sensors of optical remote sensing (fig. 3).

Sentinel-1 mission is the first and one among the five earth observation missions of European Space Agency (ESA) that are developed for Copernicus joint initiative to continue the C-band SAR Earth Observation heritage of the European Space Agency's ERS-1, ERS-2 and ENVISAT, and Canada's RADARSAT-1 and RADARSAT-2. Remote sensing from S-1 depends on transmission, reception, absorption, and direction of sensors energy. The C-band has a wavelength of 5.8 cm, which is common on many airborne research systems and space-borne systems (including IRS Oceansat-1 and RISAT) [*Aher et al.*, 2014]. The electromagnetic waves are produced by excited atoms. Every atom of a material produces the electromagnetic waves into multiple directions or multiple plain of oscillations. This type of light beam which has vibrations in more than one plain is called "Unpolarised light". If the light beam which has

vibrations in one plain is called “Polarised light”. In polarised radar, the antenna or Synthetic aperture can transmit or receive signals in either horizontal or vertical mode. Similarly, the antenna receives either the horizontally or vertically polarised backscattered energy and some radars can receive both. These two polarisation states are designated by the letters H (for Horizontal) and V (for Vertical). Thus, resulted in four combinations of polarisation effects [*Bhatta,* 2011].

Polarisation effects:

- VV — Vertical transmit, Vertical receival;
- VH — Vertical transmit, Horizontal receival;
- HH — Horizontal receival, Horizontal transmit;
- HV — Horizontal transmit, Horizontal receival.

Sentinel-1 revisit period is increased due to two factors. Firstly, due to inclusion of Terrain Observation with Progressive Scans SAR (TOPSAR) technique, resulting in a large footprint while maintaining a relatively high spectral resolution. Secondly, Sentinel-1 mission consists of two satellites (Sentinel-1A and Sentinel-2B, launched in 3rd April 2014 and 25th April 2016 respectively) which will individually record radar images for every 12 days, disregarding the weather and time of the day. The two satellites share the same orbital plane with 180° orbital phasing difference, so that temporal resolution also shared between them resulting in revisit time reduced from 6−12 days [*Yague-Martinez et al.*, 2016]. The S-1 Synthetic Aperture Radar (SAR) imaging instrument is able to switch between four sensor observation modes: Strip Map (SM), Interferometric Wide Swath (IW), Extra-Wide Swath Mode (EW) and Wave-Mode (WV) with different spatial resolutions and different swath widths. For the current work, IW mode (250 km swath width and approximately 10 m spatial resolution) was taken.

Sentinel-2 mission consists of two satellites Sentinel-2A and Sentinel-2B launched in 23rd June 2015 and 7th March 2017 respectively with orbital phasing difference of 180° to each other, with swath width of 290 da[1]. Remote sensing from S-2 depends on transmission, reception and absorption of parts of Electromagnetic spectrum, with different spatial resolutions [*Kaplan, Avdan,* 2017]. S-2 is carrying a Multi-Spectral Imaging Instrument (MSI). In S-2, all 13 spectral bands are openly accessible, unlike the S-1, in which among VV, VH, HH, HV polarised bands only VV, VH are accessible to all including other non-European citizens. Among 13 spectral bands, 4 are visible (with 10 m spatial resolution), 6 are of Near Infrared (with 20 m spatial resolution) and 3 are of Short-Wave Infrared bands (with 60 m spatial resolution). Revisit time of S-2A and S-2B together makes up revisit time of 5-10 days of revisit time.

The histogram of the imageries assists in differentiating between the water and non-water classes. Using histogram thresholding technique, backscattered (Sigma nought) distribution of pixel values of features can be differentiated with higher values of backscatter indicate non-water class and lower values indicate water class. This method of Threshold technique is one among popular methods for flood estimation [*Dadhich et al.*, 2019]. Sometimes, threshold technique is applied with morphological filtering operations, which helps in filling the gaps and holes resulting from binary mask of threshold technique [*Jo et al.*, 2018]. RGB clustering is current popular method which is easy to estimate the flood areas using RGB colour combinations *[Uddin et al.*, 2019].

Using Tasselled Cap Transformation (TCP) technique of Orthogonal transformation model from segmented Sentinel-2 images, finally classifying the flooded areas one among complicated methods currently practised [*Nedkov,* 2017]. Another method, which uses of altitude and precipitation information, is One-class classifier Bias support vector machines (BSVM). Land cover classification using Best Available Pixel (BAP) composites, times series and ecological information [*Gómez et al.*, 2016]. The chance of cloud free data over the same

[1] *Suhet.* Sentinel -2 User Handbook, European Space Agency, 2015

location increases with repeat observation. Cloud free surface reflectance composites over larger areas can be auto generated from choice-based Landsat observations. These BAPs can be produced with preferred rule-based criteria for specified applications like land cover *[Griffiths et al.*, 2013; *White et al.*, 2014]. But for the current study, RGB clustering method was explored in Sentinel-2 for flooded areas estimation. This method uses of RGB colour combinations and based on visual interpretation; the elements of the earth surface get classified.

Built-up damage assessment using coherent change detection [*Guida et al.*, 2018]. In some cases SAR simulation technique is explored besides comparing with real SAR images to mitigate distortions of the high buildings and other urban features due to occlusions in SAR images [*Balz*, 2004]. But for the current study RGB clustering from RGB colour combinations was explored, which formulates as a fastest and simplified method in built-up estimation followed by damage estimation.

There are two major techniques for built-up area extraction from satellite imagery. Firstly, techniques based on conventional multi-spectral image classification like supervised, unsupervised, object based or deep learning classification [*Ndehedehe et al.*, 2013; *Rawat, Kumar*, 2015; *Forget et al.*, 2017; *Bramhe et al.*, 2018]. Secondly, techniques based on normalised differences indices like normalised difference built-up index (NDBI), urban index (UI), enhanced built-up index (EBI), principal component analysis based built-up area index (PCABAI), etc. [*Xu*, 2007; *Kumar et al.*, 2012; *Varshney*, 2013; *Valdiviezo et al.*, 2018]. For the current built-up area estimation the RGB clustering from RGB colour combination as suggested [*Vigneshwaran, Selvaraj*, 2018] was used.

The current study is taken up with certain limitations in data and processing. First is the Data availability without same dates from S-1A and S-2B, since S-1A and S-2B are two different satellites launched in different orbits at different launching times. Second is the pre-processing of S-2B was not extended for removing the cloud cover from the imagery at least near to the cloud data due to the lack of resources in terms of software and algorithms to ensure it.

MATERIALS AND METHODS OF RESEARCHES

Entire methodology was majorly divided under five major parts. Firstly, pre-processing of both S-1A and S-2B using Snap 7.0 and Sen2Cor plugin respectively. Pre-processing is followed by flooded areas and built-up areas estimation. Later the damaged built-up and vegetation due to august 2019 east Godavari floods. The acquired results from classification were validated using random pixel distribution technique in Snap software (fig. 4).

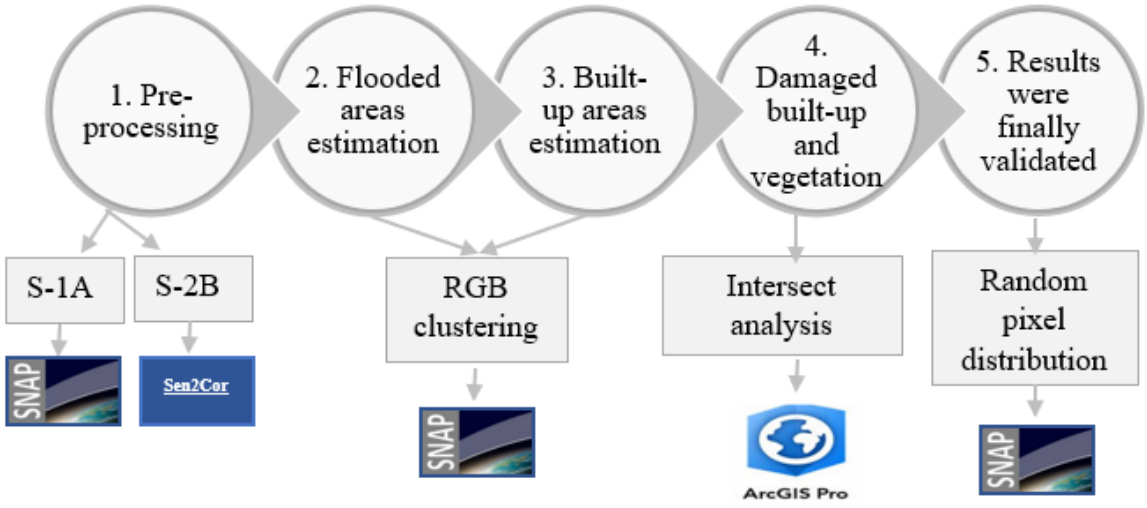

Fig. 4. Main methodology workflow

Since the current work is about comparing the estimation of S-1A and S-2B, the datasets were acquired as per the timing of two case studies of August 2019 floods in East Godavari district and Titli cyclone during October 2018 in East Godavari, Visakhapatnam and Vizianagaram district. The datasets were also acquired as per the requirements of built-up and vegetation estimations. The sources for this data acquisition are Copernicus open access hub, Alaska satellite facility and National disaster response force (table 1).

Table 1. Dates of data acquired for current work

Mission	**August Floods**	**Built-up**	**Titli Cyclone**
Sentinel-1A	Preflood: 2nd May 2019 Flood: 6th August 2019	28th September 2018 2nd May 2019	Preflood: 28th September 2018 Flood: 10th October 2018
Sentinel-2B	Preflood: 6th May 2019 Flood: 4th August 2019	6th May 2019	

Since the current study aims at differentiating flooded areas, built-up and vegetation, between microwave and optical data, S-1A and S-2B were acquired. These are openly accessible. The properties of S-1A and S-2B that were acquired for the current study are mentioned in the following (table 2).

Table 2. Properties of data that were collected

Sentinel -1A	**Sentinel -2B**
Properties: • Mission — Sentinel-1A with Synthetic Aperture Radar (SAR) imaging instrument; • Sensor acquisition mode — Interferometric wide swath mode (IW); • Resolution type — High; • Product type — Ground range detected high resolution images (GRDH); • Level of processing mode — L1; • Polarisation type — Standard Dual polarisation (SDV) =VV+VH; • Spatial resolution — 10 m; • Revisit time of together S1A & S2B range — 6−12 days	Properties: • Mission — Sentinel-2B with multispectral imaging (MSI) instrument; • Level of processing mode — L1 C; • Bands — 13 spectral bands; • Revisit time of together S2A and S2B — 5−10 days

Pre-processing of S-1A and S-2B involves in correction of the imageries to further process for specified applications. Pre-processing workflow consists of seven major methods followed as suggested here [*Filipponi*, 2019]:

1. Apply orbit file: This step corrects the orbit between mission's swath and real ground. The required orbit states vector for orbit file correction are provided within the metadata of SAR products and are not reliably accurate. The precise orbit of satellites is determined after few days and are available after the product generation.

2. Thermal noise removal: Since the S-1A and S-1B both are of active sensors; it imprints some thermal noise on imageries while transmitting and recording active microwave sensor's energy. Hence the S-1A and S-1B imageries' intensity is disturbed by the additive thermal noise, especially in the cross-polarized channel [*Park et al.*, 2017].

3. Calibration to Sigma 0: Since the values recorded in the datasets are not easy interpretable, all the backscattered energy that got recorded by the sensor gets calibrated to sigma 0 values, which are interpretable by the successive processing algorithms.

4. Speckle removal: Speckle is like a granular or salt and pepper noise in SAR imageries due to the interference of waves [*Lee et al.*, 1994]. Lee filter with window size of 7*7 was applied to remove the speckle in S-1A imageries.

5. Slice Assembly: Since the current data are in one orbit, the swaths collected can be just assembled. That's the reason why the mosaic technique is not applied for current study area extraction from multiple swaths.

6. Range Doppler Terrain Correction: The SAR sensor of S-1A or S-1B records the data in right looking orientation, and hence the data also looks like a mirror image of real world. The range doppler terrain correction is applied to correct the imagery orientation from sensor's orientation to earth's orientation.

7. Mask out to study area: Finally, the data was masked out to the study area, using respective study area boundaries.

Sen2Cor plugin:

- Sen2Cor is a Level-2A processor, for which the main purpose is to correct single-date S-2 Level-1C Top-Of- Atmosphere (TOA) products from the effects of the atmosphere and to deliver Level-2A Bottom-Of-Atmosphere (BOA) reflectance product. Other products generated by the Sen2Cor plugin are Aerosol Optical Thickness (AOT) map, a water vapour (WV) map and a Scene Classification (SCL) map with quality indicators for cloud and snow probabilities [*Main-Knorn et al.*, 2017].
- Sen2Cor plugin workflow consists of five modules coordinating interactions within the workflow. The Scene Classification (SCL) and Atmosphere correction (AC) modules are specially designed for processing the S-2 Level-1C input data into Level-2A products.

The main processing workflow consists of five following methods [*Gascon et al.*, 2017]:

1. Cloud Detection: to detect the cloud cover, which later used for removing the cirrus cloud.

2. Scene Classification (SCL): to classify the input S-1C data into 11 classes viz., vegetation, soils, cirrus class, water, snow, cloud shadows, dark area pixels, unclassified saturated or defective pixels including 2 classes for cloud probabilities (medium, high).

3. Retrieval of Aerosol Optical Thickness (AOT): to retrieve the aerosols values from Level-1C data and then measure for the visual transparency of the atmosphere.

4. Retrieval of Water vapor (WV): to retrieve the water vapour values from the Level-1C for which the Atmospheric Pre-corrected Differential Absorption algorithm will be used.

5. Conversion of TOA to BOA: The values of Top of the Atmosphere (TOA) will be calibrated to Bottom of the Atmosphere (BOA) which helps is analysing what is on the earth's surface, by neglecting the values reflected from top of the atmosphere.

6. Finally, the results obtained were multi-size mosaiced (since that bands of S-2B were of multiple spatial resolutions) and masked out to the study area.

The RGB clustering is the most common technique for data compression and iso-clustering works better on an optimal number of classes usually unknown [*Komac*, 2006; *Mohamed, Verstraeten*, 2012]. The RGB clustering functions are a simple classification algorithm that quickly compresses a three-band image into a single-band pseudo-colour image without necessarily classifying any particular features and without a signature file and decision rule. The RGB clustering provides greater control over the parameters used to partition the pixels into similar classes [*Kumar et al.*, 2016; *Mahi et al.*, 2016]. After exploring for RGB clustering, random forest classification technique was used to classify image into flooded and non-flooded areas. Random forest classification over maximum likelihood was chosen supervised classification of specified classes. Since RF method ensures a unique predictive validity and

model interpretability within known machine learning methods [*Horning*, 2010; *Clement et al.*, 2017].

Only VV band was explored for the built-up estimation from S-1A as suggested here [*Deepthi et al.*, 2018]. The RGB colour combination of NIR, Red, NIR bands for built-up in S-2B was explored as suggested here [*Vigneshwaran, Selvaraj*, 2018].

RESULTS OF RESEARCHES AND THEIR DISCUSSION

Samples of flooded areas were taken from the RGB colour combination result. So whichever the areas appeared in bright red colour channel, those are considered as training samples for flooded areas. Along with flooded areas, samples of waterbodies were taken from the areas of dark black colour and finally remaining areas were considered as samples for non-flooded areas. With these training samples, RF supervised classification was computed to estimate the flooded areas out of S-1A RGB colour combination (fig. 5) and S-2B (fig. 6) respectively. Flooded area of august 2019 East Godavari floods was estimated as 600.806251 km^2. The Non-flooded areas were estimated as 9748.992449 km^2 and waterbodies estimated as 440.793296 km^2.

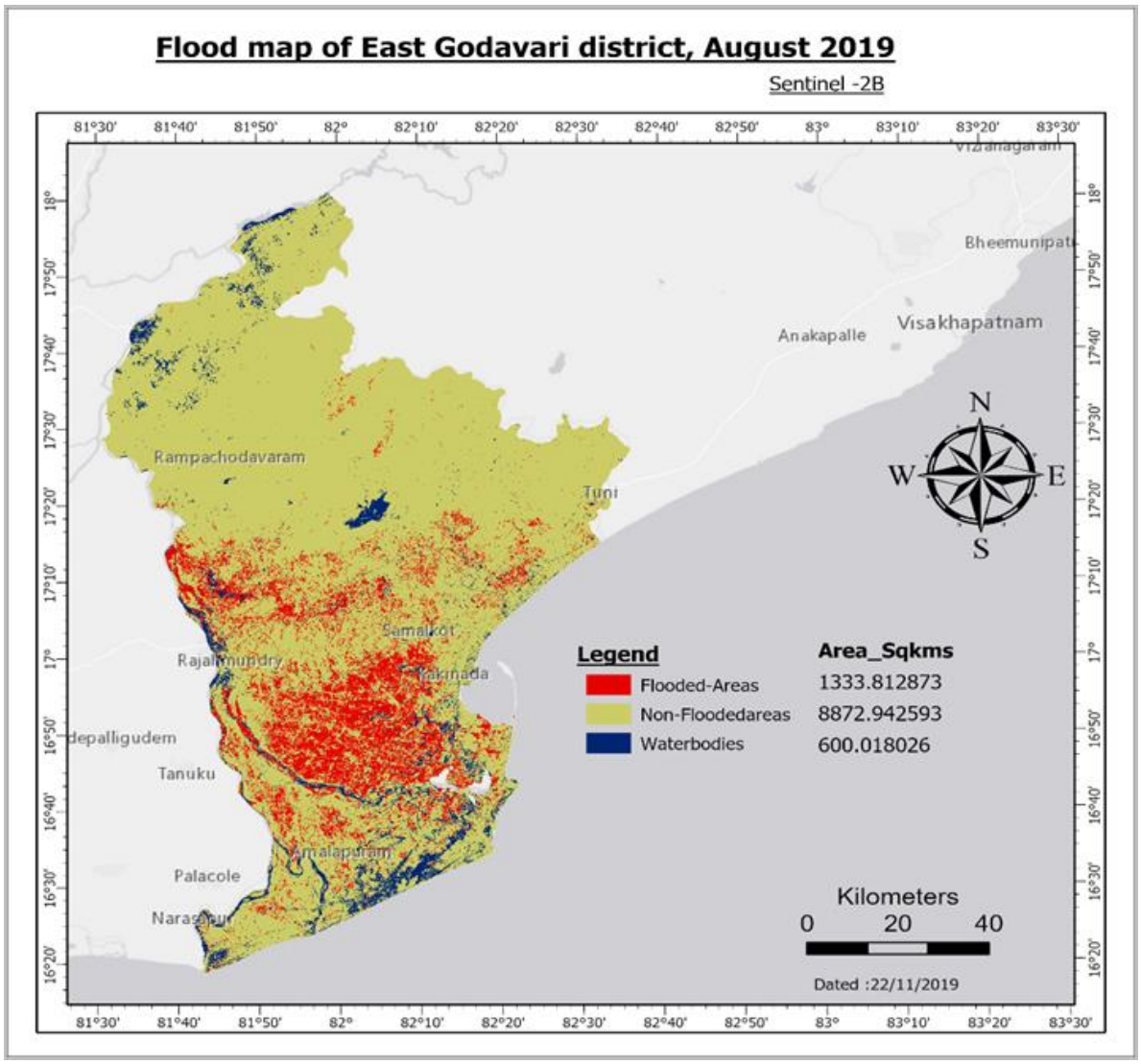

Fig. 5. Area under flood due to august 2019 EG floods, i.e., estimated in S-2B is 1333.812873 km^2

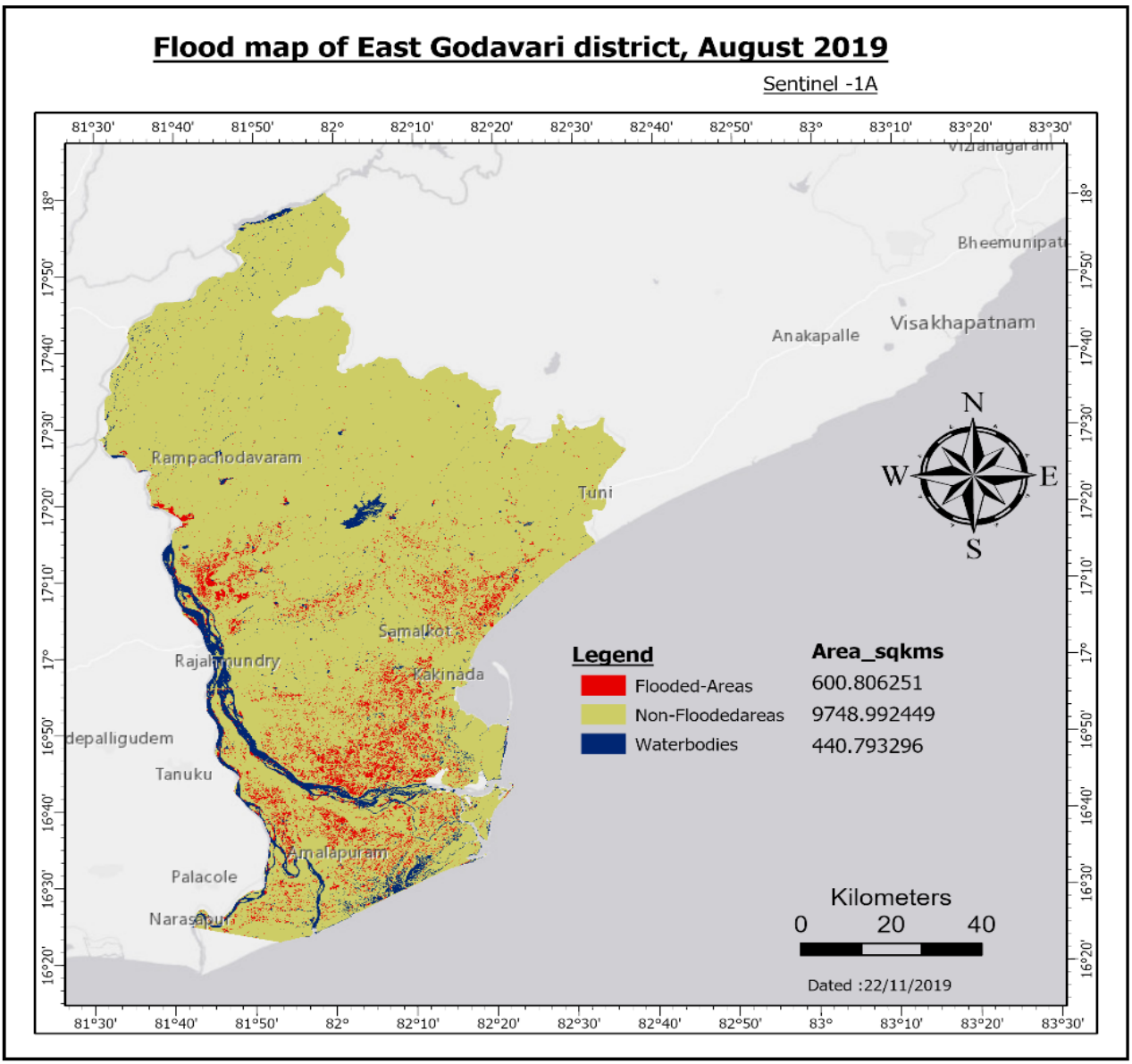

Fig. 6. Flood map of East Godavari, August 2019 from S-2B, i.e., estimated was 600.806251 km^2

Samples of built-up areas were taken from different RGB colour combination result by altering the RGB colour channels and using Google Earth. The areas appeared in red colour channel considered as training samples for built-up areas. Along with built-up areas, samples of vegetation from green colour channel and water body samples from dark black colour were taken. The RF supervised classification was computed to estimate the built-up areas out of S1-A RGB colour combination (fig. 7) and (fig. 8) respectively. Built-up map of East Godavari, 2018 from S-1A i.e., estimated was 1276.094558 and from S-2B (2018) estimated was 500.305358 km^2.

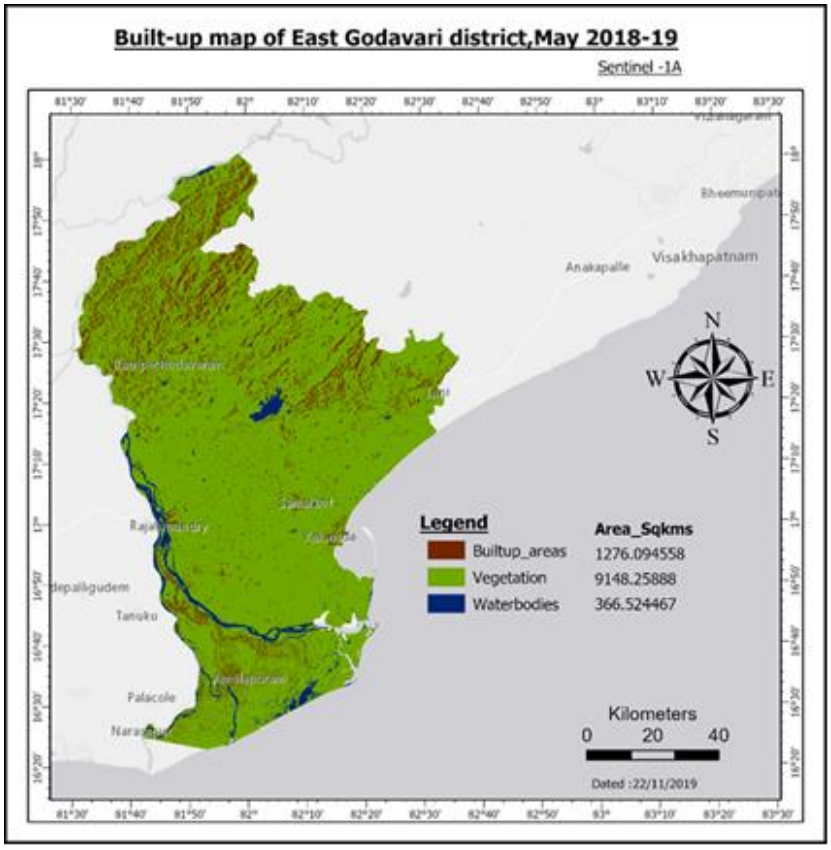

Fig. 7. Built-up map of East Godavari, 2018 from S-1A, i.e., estimated was 1276.094558 km^2

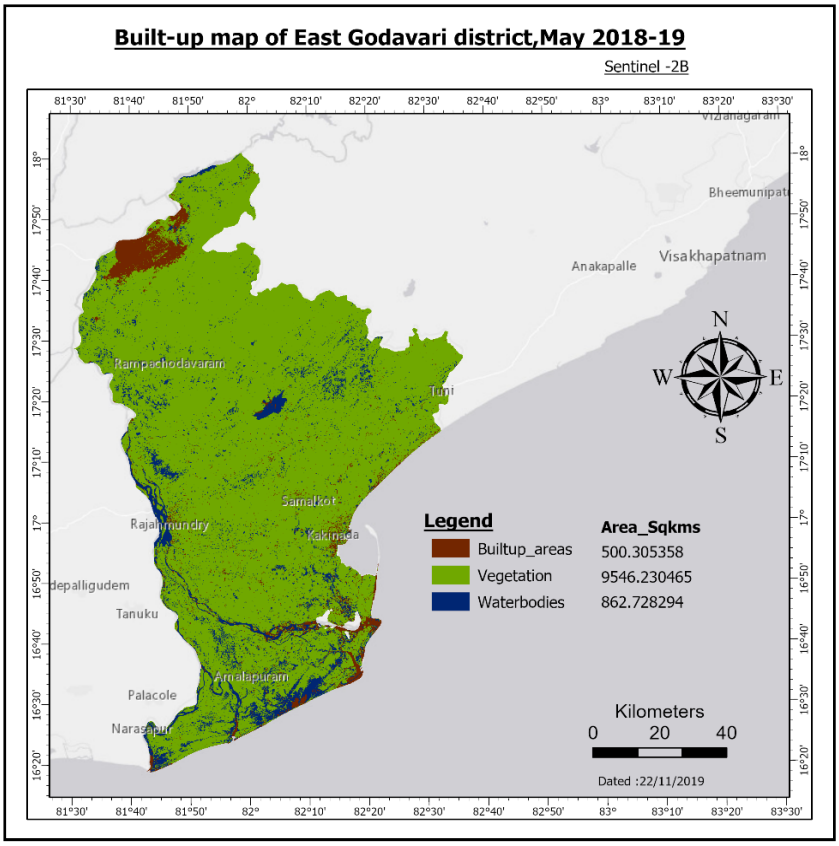

Fig. 8. Built-up map of East Godavari, 2018 from S-2B, i.e., estimated was 500.305358 km^2

CONCLUSIONS

The RGB clustering through RGB colour combination is basic method finally adopted after exploration among the fast computing methods which assists in fast computation and estimation of the flooded areas and estimation of the damaged built-up and vegetation areas due to the august 2019 East Godavari floods, India. Before applying the RGB clustering for the S-2B imageries, pre-processing is a major requirement, since the S-2B is not resistant from atmospheric and weather disturbances while recording the energy from the surface of the earth. Sen2Cor plugin was used for fast pre-processing of the S-2B imageries.

In S-2B the flooded area estimated was high than S-1A. Decentralisation to the level of sub-districts or mandals of East Godavari district was performed. The observation made here is the districts lied at the banks of the Godavari river, has low flood area estimation in S-1A and high flood area estimation in S-2B. The reason could be the gap of the two days late acquisition by S-1A and early data record by the S-2B. Hence, the limitation here would be the availability of the S-1A data during the occurrence of the flood but not two or few days later the event. Otherwise, S-2B would be preferred over S-1A. Because, S-2B data may be available during the floods and it gives approximate aerial extent of floods.

In terms of built-up area estimation, S-1A has higher area than S-2B. Decentralisation to the level of sub-districts or mandals is performed to analyse which are the areas might get classified as built-up area in S-1A built-up area estimation. The observation made from this decentralisation is that the sub-districts which has the high land cover of the fallow lands and dry lands over the mountainous areas also got classified as built-up areas in S-1A. Hence, this current work should be extended towards the delineation of the fallow lands and drylands from the built-up areas in S-1A for accurate built-up area estimation.

Further outlook:

- This work could be further extended towards careful exploration for the training samples collection in S-1A, since in our current work parts of fallow lands and dry lands were classified as built-up areas.
- What could be the changes in estimations of built-up, vegetation, and flooded areas would be with cloud free Sentinel -2B data.
- Differentiating on same dates data of S-1A and S-2B.
- Currently only the flooded area was estimated, but the quantitative analysis of flood depth also needed to explore [*Jo et al.*, 2018]. Because depth of the flood water formulates more crucial part for disaster rescue teams to evacuate people and to plan rescue operations.

REFERENCES

1. *Aher S.P., Khemnar S.B., Shinde S.D.* Synthetic aperture radar in Indian remote sensing. International Journal of Applied Information Systems, 2014. V. 7. No 2. P. 41−44.

2. *Balz T.* SAR simulation based change detection with high-resolution SAR images in urban environments. International Archives of Photogrammetry and Remote Sensing, Istanbul, 2004. V. 35. Part B.

3. *Bhatta B.* Remote sensing and GIS (2nd edition). India: Oxford University Press, 2011. 752 p.

4. *Bramhe V., Ghosh S.K., Garg P.K.* Extraction of built-up areas using convolutional neural networks and transfer learning from Sentinel-2 satellite images. The International Archives of the Photogrammetry, Remote Sensing and Spatial Information Sciences, 2018. V. 3. P. 79–85. DOI: 10.5194/isprs-archives-XLII-3-79-2018.

5. *Clement M.A., Kilsby C.G., Moore P.* Multi-temporal synthetic aperture radar flood mapping using change detection. Journal of Flood Risk Management, 2017. No 4. P. 152–168. DOI: 10.1111/jfr3.12303.

6. *Dadhich G., Miyazaki H., Babel M.* Applications of Sentinel-1 synthetic aperture radar imagery for floods damage assessment: A case study of Nakhon Si Thammarat, Thailand. The International Archives of the Photogrammetry, Remote Sensing and Spatial Information

Sciences, 2019. V. XLII-2/W13. P.1927−1931. DOI: https://doi.org/ 10.5194/isprs-archives-XLII-2-W13-1927-2019.
7. *Deepthi R., Ravindranath S., Raj G.K.* Extraction of urban footprint of bengaluru city using microwave remote sensing. The International Archives of the Photogrammetry, Remote Sensing and Spatial Information Sciences, 2018. V. XLII-5. P. 735–740. DOI: 10.5194/isprs-archives-XLII-5-735-2018.
8. *Filipponi F.* Sentinel-1 GRD preprocessing workflow. 3rd International Electronic Conference on Remote Sensing. Rome, Italy, 2019. V. 48. DOI: 10.3390/ECRS-3-06201.
9. *Forget Y., Linard C., Gilbert M.* Automated supervised classification of Ouagadougou built-up areas in Landsat scenes using OpenStreetMap. Conference: Joint Urban Remote Sensing Event, Dubai, 2017. No 3. DOI: 10.1109/JURSE.2017.7924571.
10. *Gascon F., Bouzinac C., Thépaut O., Jung M., Francesconi B., Louis J., Lonjou V., Lafrance B., Massera S., Gaudel-Vacaresse A., Languille F., Alhammoud B., Viallefont F., Pflug B., Bieniarz J., Clerc S., Pessiot L., Trémas T., Cadau E., Bonis R.D., Isola C., Martimort M., Fernandez V.* Copernicus Sentinel-2A calibration and products validation status. Remote Sensing, 2017. V. 9. 584 p.
11. *Gómez C., Michael A.W., Wulder., White J.C.* Optical remotely sensed time series data for land cover classification: A review. International Society for Photogrammetry and Remote Sensing, Journal of Photogrammetry and Remote Sensing, 2016. V. 116. P. 55–72. DOI: 10.1016/j.isprsjprs.2016.03.008.
12. *Griffiths P., Linden S., Kuemmerle T., Hostert P.* A pixel-based Landsat compositing algorithm for large area land cover mapping. IEEE Journal of Selected Topics in Applied Earth Observations and Remote Sensing, 2013. V. 6. P. 2088–2101.
13. *Guida L., Boccardo P., Donevski I., Schiavo L.L., Molinari M.E., Monti-Guarnieri A., Oxoli D., Brovelli M.A.* Post-disaster damage assessment through coherent change detection on sar imagery. The International Archives of the Photogrammetry, Remote Sensing and Spatial Information Sciences, 2018. V. 3. P. 431–436.
14. *Horning N.* Random Forests: An algorithm for image classification and generation of continuous fields datasets. International Conference on Geoinformatics for Spatial Infrastructure Development in Earth and Allied Sciences, Osaka, 2010. V. 911. P. 1−6.
15. *Jain R.K.* "Cyclone Hudhud". Strategies and Lessons for Preparing Better & Strengthening Risk Resilience in Coastal Regions of India. National Disaster Management Authority, 2015. 58 p.
16. *Jo M.J., Osmanoglu B., Zhang B., Wdowinski S.* Flood extent mapping using dual-polarimetric Sentinel-1 synthetic aperture radar imagery. The International Archives of the Photogrammetry, Remote Sensing and Spatial Information Sciences, 2018. V. 3. P. 711−713. DOI: 10.5194/isprs-archives-XLII-3-711-2018.
17. *Joyce K.E., Belliss S.E., Samsonov S.V., McNeill J.S., Glassey J.P.* A review of the status of satellite remote sensing and image processing techniques for mapping natural hazards and disasters. Progress in Physical Geography, 2009. V. 33. P. 183–207. DOI: 10.1177/0309133309339563.
18. *Kaplan G.J., Avdan U.* Object-based water body extraction model using Sentinel-2 satellite imagery. European Journal of Remote Sensing, 2017. V. 50. No 1. P. 137−143. DOI: 10.1080/22797254.2017.1297540.
19. *Klemas V. V.* The role of remote sensing in predicting and determining coastal storm impacts. Journal of Coastal Research, 2009. V. 25. P. 1264–1275. DOI: 10.2112/08-1146.1
20. *Komac M.* A landslide susceptibility model using the analytical hierarchy process method and multivariate statistics in perialpine Slovenia. Geomorphology, 2006. V. 74. P. 17–28. DOI: 10.1016/j.geomorph.2005.07.005.

21. *Kumar A., Pandey A.C., Jeyaseelan A.T.* Built-up and vegetation extraction and density mapping using WorldView-II. Geocarto International, 2012. V. 27. P. 557–568. DOI: 10.1080/10106049.2012.657695.
22. *Kumar G., Sarthi P.P., Ranjan P., Rajesh R.* Performance of k-means based satellite image clustering in RGB and HSV color space. International Conference on Recent Trends in Information Technology (ICRTIT), Chennai, India. 2016. P. 1–5. DOI: 10.1109/ICRTIT.2016.7569523.
23. *Lee J.S., Jurkevich L., Dewaele P., Wambacq P., Oosterlinck A.* Speckle filtering of synthetic aperture radar images: A review. Remote Sensing, 1994. V. 8. P. 313–340.
24. *Mahi H., Farhi N., Labed K.* Unsupervised classification of satellite images using K-Harmonic means algorithm and cluster validity index. EARSeL eProc, 2016. V. 15. 10 p. DOI: 10.12760/01-2016-1-02.
25. *Main-Knorn M., Pflug B., Louis J., Debaecker V., Müller-Wilm U., Gascon F.* Sen2Cor for Sentinel-2. Image and Signal Processing for Remote Sensing XXIII, Germany, 2017. SPIE Proceedings. V. 10427. 12 p. DOI: 10.1117/12.2278218.
26. *Mohamed I.N.L, Verstraeten G.* Analyzing dune dynamics at the dune-field scale based on multi-temporal analysis of Landsat-TM images. Remote Sensing of Environment, 2012. V. 119. P. 105–117. DOI: 10.1016/j.rse.2011.12.010.
27. *Ndehedehe C.E., Oludiji S.M., Asuquo I.M.* Supervised learning methods in the mapping of built up areas from Landsat-based satellite imagery in part of Uyo Metropolis. New York Science Journal, 2013. V. 6. P. 45–52.
28. *Nedkov R.* Orthogonal transformation of segmented images from the satellite Sentinel-2. Comptes Rendus de l'Academic Bulgare des Sciences, 2017. V. 70. P. 687–692.
29. *Park J.W., Korosov A., Babiker M.* Efficient thermal noise removal of Sentinel-1 image and its impacts on sea ice applications. EGU General Assembly Conference Abstracts, Vienna, Austria, 2017. P. 12613.
30. *Pradesh A.* Flood situation in Godavari delta still grim. The Hindu. Delhi, 2019. No 8. Electronic resource: https://www.thehindu.com/news/national/andhra-pradesh/flood-situation-in-godavari-delta-still-grim/article28816309.ece (accessed 05.05.2020).
31. *Rawat J.S., Kumar M.* Monitoring land use or cover change using remote sensing and GIS techniques: A case study of Hawalbagh block, district Almora, Uttarakhand, India. Egyptian Journal of Remote Sensing and Space Sciences, 2015. V. 18. P. 77−84. DOI: 10.1016/j.ejrs.2015.02.002.
32. *Saptarsi G., Ghosh S., Chakrabarti A., Chakraborty B., Chakraborty S.* A review on application of data mining techniques to combat natural disasters. Ain Shams Engineering Journal, 2018. V. 9. P. 365 –378. DOI: 10.1016/j.asej.2016.01.012.
33. *Uddin K., Matin M.A., Meyer F.J.* Operational flood mapping using multi-temporal Sentinel-1 SAR images: A case study from Bangladesh. Remote Sensing, 2019. V. 11 (13). P. 1518. DOI: 10.3390/rs11131581.
34. *Valdiveizo-N J.C., Salazar-G A., López-C A.A.* Built-up index methods and their applications for urban extraction from sentinel 2A satellite data: discussion. Optical Society of America, 2018. V. 35. N 1. P. 35−44. DOI: 10.1364/JOSAA.35.000035.
35. *Varshney A.* Improved NDBI differencing algorithm for built-up regions change detection from remote sensing data: An automated approach. Remote Sensing Letters, 2013. V. 4. P. 504−512. DOI: 10.1080/2150704X.2013.763297.
36. *Vigneswaran S., Selvaraj V.K.* Extraction of built-up area using high resolution Sentinel-2A and google satellite imagery. International Archives of the Photogrammetry, Remote Sensing and Spatial Information Sciences, 2018. V. XLII-4/W9. P. 165−169. DOI: 10.5194/isprs-archives-XLII-4-W9-165-2018.
37. *White J.C., Wulder M.A., Hobart G.W., Luther J.E., Hermosilla T., Griffiths P., Coops N.C., Hall R.J., Hostert P., Dyk A., Guindon L.* Pixel-based image compositing for large-area dense

time series applications and science. Canadian Journal of Remote Sensing, 2014. V. 40. P. 192–212. DOI: 10.1080/07038992.2014.945827.
38. *Xu X.* Extraction of urban built-up land features from Landsat imagery using a thematic-oriented index combination technique. Photogrammetric Engineering and Remote Sensing, 2007. V. 73. No 12. P. 1381−1391.
39. *Yague-Martinez N., Prats-Iraola P., Gonzalez F.R., Brcic R., Shau R., Geudtner D., Eineder M., Bamler R.* Interferometric processing of Sentinel-1 TOPS data. EEE Transactions on Geoscience and Remote Sensing, 2016. V. 54. P. 2220–2234. DOI: 10.1109/ TGRS.2015.2497902.